

Use of total variation filters in SPECT medical imaging

Author: Idoia Ruiz López.

Advisors: Artur Carnicer, Ignasi Juvells.

Facultat de Física, Universitat de Barcelona, Diagonal 645, 08028 Barcelona, Spain.

Abstract: Total variation denoising filtering is proposed as an alternative to the Butterworth filter, which is widely used in the reconstruction of SPECT medical images. Its advantages lie in the preservation of the image edges while the noise is removed, as opposed to the blurring that characterizes Butterworth filtered images. However, results show that total variation filtering application to SPECT medical images doesn't represent an improvement in terms of similarity to the reference image.

I. INTRODUCTION

In order to use SPECT medical images as a diagnosis tool, a proper denoising process is required, due to the low signal to noise ratio of this kind of images, caused by the small amount of detected photons and their scattering that degrades the images increasing their noise.

A Butterworth filter is commonly used for this purpose. However, its denoising effects carry a blurring of the image. It softs the edges of the image, as well as the noise, as they both come from the high frequency information of the image that is what a Butterworth filter removes.

As opposed, Total Variation denoising filtering is characterized by the preservation of the image discontinuities. In this study we will compare the results of applying these two denoising methods.

II. METHODS

A. Filtered back projection with Butterworth filter

The filtered back projection (FBP) consist in recovering the image $f(x,y)$ from a set of projections $p_\theta(t)$ from different angles θ that cover a full rotation. The image can be obtained doing the back projection (1) of the filtered projections,

$$f(x,y) = \int_0^\pi p'_\theta(x\cos\theta + y\sin\theta)d\theta \quad (1)$$

where $p'_\theta(t)$ are the projections filtered by the ramp filter (the result of multiplying in the Fourier domain the Fourier transform of the projections $p_\theta(t)$ with the ramp filter $|\omega|$, as shown in equation (2))

$$p'_\theta(t) = \int_{-\infty}^{\infty} P_\theta(\omega)e^{i2\pi\omega t}|\omega|d\omega \quad (2)$$

where $P_\theta(\omega)$ is the Fourier transform of the projection $p_\theta(t)$ at angle θ .

Summarizing, for each of the projections $p_\theta(t)$, we have to calculate its Fourier transform $P_\theta(\omega)$, then multiply it with the ramp filter $|\omega|$, and do the inverse Fourier transform to get the filtered projections $p'_\theta(t)$. Finally, we do the back projection (1).

For a deeper explanation of FBP and the detailed derivation, refer to [4].

We have considered two approaches for applying the Butterworth filter. The first one consist in applying it on the two dimensional projections before the FBP reconstruction. The second one is to include it in the FBP. The Butterworth

filter can be included in the FBP multiplying the ramp filter as shown in equation (3)

$$p'_\theta(t) = \int_{-\infty}^{\infty} P_\theta(\omega)e^{i2\pi\omega t}|\omega| \frac{1}{\sqrt{1 + \left(\frac{\omega}{\omega_{cutoff}}\right)^{2N}}}d\omega \quad (3)$$

The Butterworth filter cuts the image signal above a certain cutoff frequency ω_{cutoff} (how sharp is the cutting depends on the order N of the filter). Therefore, the high frequency information of the image, such as the noise as well as the image details like the edges, is being removed.

B. Proposed Total Variation filtering

Total Variation (TV) denoising filtering was introduced by Rudin, Osher and Fatemi [1]. Its basic idea consists in the minimization of the total variation of the image maintaining the similarity to the original image (4).

$$\min_y TV(y) + \frac{\lambda}{2} \int (f(x) - y(x))^2 dx \quad (4)$$

where $TV(y)$ is the total variation of the image that can be defined as

$$TV(y) = \|y\|_{TV} \approx \sum_{i,j} \sqrt{|y_{i,j} - y_{i-1,j}|^2 + |y_{i,j} - y_{i,j-1}|^2}$$

where y_{ij} are the image values of the denoised image y . f is the original image and λ is a positive parameter that controls the denoising weight against the similarity to the original image. As λ is chosen greater, the differences between the denoised and original image tend to be more strongly minimized than the total variation of the denoised image, which will be less denoised but more similar to the original one.

We have used the Split Bregman algorithm [2][3], which is implemented in the scikit-image Python library.

The reason why TV filtering seems an attractive alternative is because the main characteristic of TV denoised images is the preservation of the sharpness of the image edges as opposed to the Butterworth filter which smoothing blurs the discontinuities.

We will perform TV denoising combined with the FBP using only its implicit ramp filter. As in the previous method, two approaches have been considered. In the first one, TV denoising will be applied on the two dimensional projections before the FBP. The second approach consists in applying it after the FBP, on the reconstructed image.

III. FIGURE OF MERIT

In order to perform a quantitative comparison between the different methods, we will use the Pearson correlation coefficient as a figure of merit.

The Pearson correlation coefficient measures the linear correlation between two sets of data, in our case, the reconstructed images and the synthetic phantom reference images. It can be defined as

$$r = \frac{\sum (x_i - \bar{x})(y_i - \bar{y})}{\sigma_x \sigma_y}$$

where x_i and y_i are the values of the compared images, \bar{x} and \bar{y} are their means, and σ_x and σ_y are their standard deviation.

IV. RESULTS

The behaviour of the photons in SPECT imaging has been simulated with a Monte Carlo method from a phantom, giving us realistic noisy projections, with which we have performed the reconstruction of the images using the described methods in section II. These projections have been provided by the Biophysics and Bioengineering Unit from the Biomedicine Department of the University of Barcelona.

We have 120 projections (with a size of 128x54) acquired from different angles that complete a 360° rotation. Therefore, the three dimensional phantom is composed by 54 axial slices, each one having a size of 128x128. For the analysis we have only considered the slices from 3 to 45 due to the lack of data in the first and last ones.

The images obtained corresponding to the axial slice 22 of the phantom are shown in Fig. (1), and the horizontal profiles of a central row of the images are shown in Fig. (2).

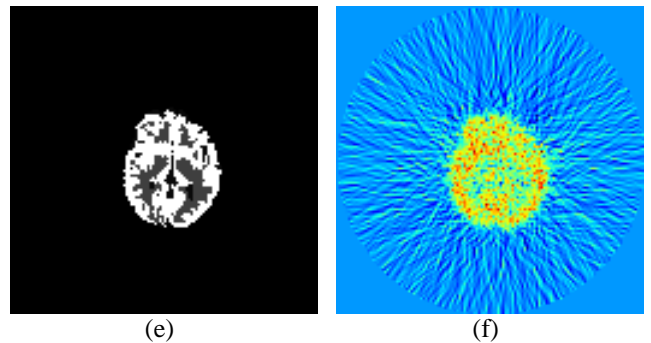
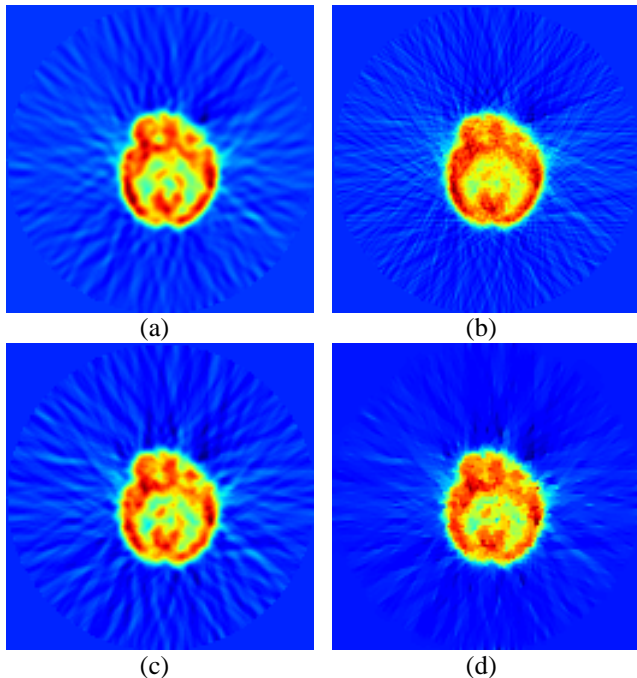


FIG. 1: Comparison between the reconstructed images of the phantom axial slice 22 obtained using the following filters, shown with a ‘jet’ colour map. (a) Butterworth filter (cutoff frequency: 0,17, order: 2,9) on the projections before FPB. (b) TV filter (λ : 0,24) on the projections. (c) Butterworth filter (cutoff frequency: 0,9, order: 2,9) used in the FBP multiplying the ramp filter. (d) TV filter (λ : 4,28) on the image reconstructed by FBP using only the ramp filter. (e) Phantom. (f) Only the ramp filter of the FBP.

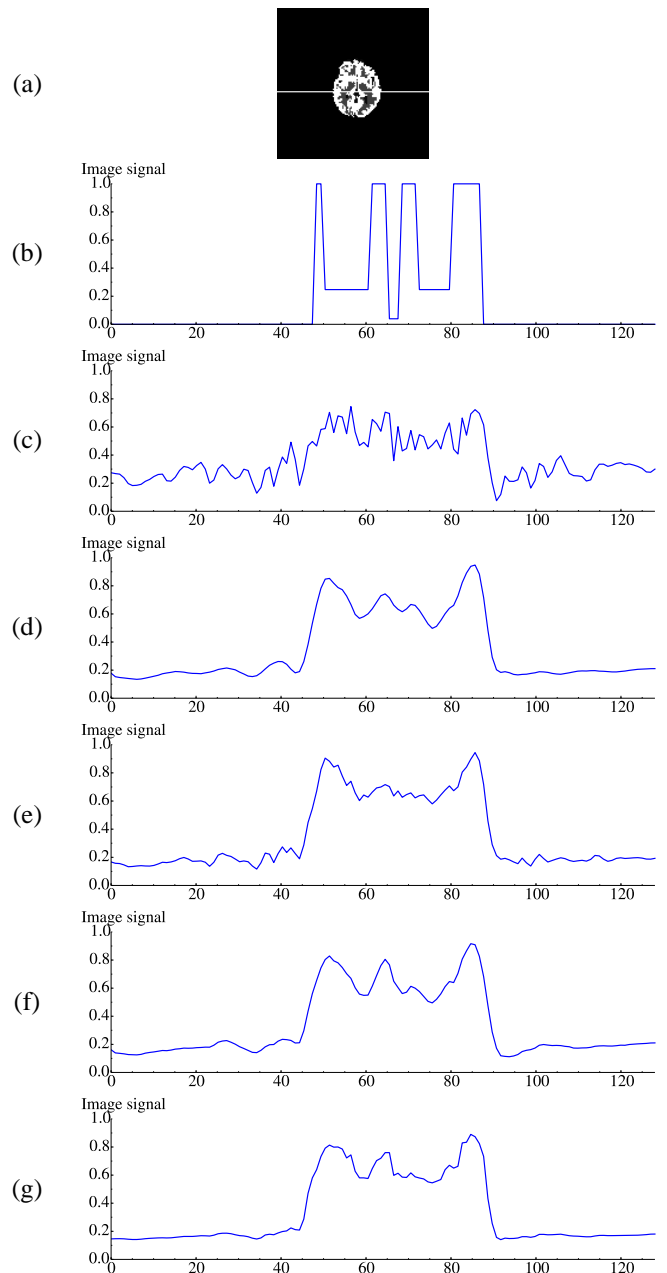


FIG. 2 Horizontal profile of the row 70 (shown in (a)) of the reconstructed image, corresponding to the axial slice 22, obtained by using: (b) Phantom. (c) Only the ramp filter in FBP. (d) Butterworth filter (cutoff frequency: 0,17, order: 2,9) on the projections. (e) TV filter (λ : 0,24) on the projections. (f) Butterworth filter (cutoff frequency: 0,9, order: 2,9) used in the FBP multiplying the ramp filter. (g) TV filter (λ : 4,28) on the image reconstructed by FBP using only the ramp filter

Fig.(1) shows that Butterworth filtered images are smoother than those obtained by TV. However, they have a higher contrast. This is clearly shown in Fig.(2), since the intensity differences in the profile are smaller. It is also shown in Fig.(2) that TV filtered images have a “staircase” effect while Butterworth images have a continuous profile. This effect causes the image to look sharper while the Butterworth image looks more blurred. Comparing them with the phantom reference image, it may be observed that this sharpness does not involve a better quality of the image as it is countered by the low contrast as well as the low resolution of SPECT images, that makes more difficult to recover the image details. These two TV filtering drawbacks were already noticed in [3].

In order to compare the goodness of the obtained images, we have calculated the Pearson correlation coefficient for all of the axial slices of the phantom, as shown in Fig.(3). The Butterworth filtering on the projections before the FBP has slightly higher correlation. However, the differences between the correlation coefficients of the different methods are non-significant. The numeric values for the slice 22 are shown in the Table (I).

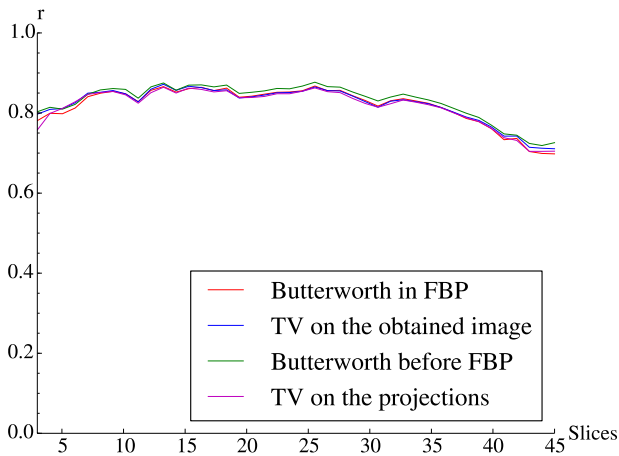


FIG. 3 Pearson correlation coefficient for every axial slice obtained by the described methods in section II.

Filter type	Pearson correlation coefficient
Butterworth before FBP	0,861
TV on the projections	0,848
Butterworth in FBP	0,852
TV on the reconstructed image	0,851

TABLE I: Pearson correlation coefficient of the obtained images that correspond to the axial slice 22 of the phantom.

V. CONCLUSIONS

- The use of TV filtering in SPECT medical imaging provide sharper images with a lower contrast than those obtained by the Butterworth filter. The overall effect does not involve a better quality of the image, since the loss of contrast counters the preservation of the image discontinuities. We shall conclude that in comparison with the Butterworth filter, TV denoising in SPECT images does not represent an improvement of the obtained images in terms of similarity to the reference images, that has been measured by the Pearson correlation coefficient, showing that there are not significant differences between both methods.

Acknowledgments

I would like to express my gratitude to my advisors A. Carnicer and I. Juvells for giving me the opportunity to do this project as well as for their valuable advices and knowledge. I also would like to thank the Biophysics and Bioengineering Unit from the Biomedicine Department of the University of Barcelona for their collaboration providing us the phantom and the simulated images that have allow us to perform this study. Finally, I would like to thank my family the given support during all these years.

[1] L. Rudin, S. Osher, and E. Fatemi, «Nonlinear total variation based noise removal algorithms,» *Physica D.*, vol. 60, pp. 259-268, 1992.

[2] T. Goldstein and S. Osher, «The Split Bregman Method For L1 Regularized Problems,» *SIAM J Imaging Sci.*, vol. 2, pp. 323-343, 2009.

[3] P. Getreuer, «Rudin–Osher–Fatemi Total Variation Denoising using Split Bregman,» *Image Processing On Line*, vol.2, pp. 74-95, 2012.

[4] A. C. Kak and M. Slaney, «Principles of Computerized Tomographic Imaging,» *IEEE Press*, pp. 60-75, 1988